Citation
Ciampi, S. and Darwish, N. and Aitken, H. and Díez-Pérez, I. and Coote, M. 2018. Harnessing electrostatic catalysis in single molecule, electrochemical and chemical systems: a rapidly growing experimental tool box. Chemical Society Reviews. 47: pp. 5146-5164. http://doi.org/10.1039/c8cs00352a

Journal Name

ARTICLE

Harnessing Electrostatic Catalysis in Single Molecule, Electrochemical and Chemical Systems: A Rapidly Growing Experimental Tool Box

Received 00th January 20xx,
Accepted 00th January 20xx

DOI: 10.1039/x0xx00000x

www.rsc.org/

Simone Ciampi,[†,*a] Nadim Darwish,[†,*a] Heather M. Aitken, [†,b] Ismael Diez Perez[c] and Michelle L. Coote*[b]

Static electricity is central to many day-to-day practical implications, from separation methods in the recycling of plastics to transfer inks in photocopying, but the exploration of how electrostatics affects chemical bonding is still in its infancy. As shown in the Companion Tutorial, the presence of an appropriately-oriented electric field can enhance the resonance stabilization of transition states by lowering the energy of ionic contributors, and the effect that follows on reaction barriers can be dramatic. However, the electrostatic effects are strongly directional and harnessing them in practical experiments has proven elusive until recently. This tutorial outlines some of the experimental platforms through which we have sought to translate abstract theoretical concepts of electrostatic catalysis into practical chemical technologies. We move step-wise from the nano to the macro, using recent examples drawn from single-molecule STM experiments, surface chemistry and pH-switches in solution chemistry. The experiments discussed in the tutorial will educate the reader in some of the viable solutions to gain control of the orientation of reagents in that field; from pH-switchable bond-dissociations using charged functional groups to the use of surface chemistry and surface-probe techniques. All of these recent works provide proof-of-concept of electrostatic catalysis for specific sets of chemical reactions. They overturn the long-held assumption that static electricity can only affect rates and equilibrium position of redox reactions, but most importantly, they provide glimpses of the wide-ranging potential of external electric fields for controlling chemical reactivity and selectivity.

Key Learning Points

(1) Three practical strategies –from the nano to the macro scale – to harness electric fields as effectors of chemical change are outlined:
- use of oriented-external electric fields (OEEFs) in single-molecule scanning tunnelling microscopy (STM) experiments in solvents of low dielectric.
- use monolayer-modified electrodes to probe electrical double layer and semiconductors space-charge to deliver interfacial electric fields (IEFs)
- use of designed local electric fields (D-LEFs) from charged functional groups

(2) For each platform, the theoretical background is explained, prototypical examples are outlined, and practical guidance on maximizing catalysis and avoiding interference from unwanted processes is provided.
(3) Future outlook and imagined potential of the field, including probing the EF effects in enzymatic catalysis.
(4) Critical discussions of the underlying theory of electrostatic effects on chemical reactions, their directionality and factors affecting their magnitude can be found in the companion Tutorial Review

1. Introduction

Chemical reactions are often classified into redox and non-redox processes. Chemists appreciate that redox reactions respond predictably to changes in voltage – a bias of about 1 Volt can ordinarily lead to changes in redox currents by a factor of up to 10^8.[1] These currents are the manifestation of the rate at which electrons are exchanged (i.e. lost or gained) at an electrified interface, hence the field-effect is easily explained and accounted for. On the other hand, the impact of an external electric field on non-redox reactivity and selectivity, long anticipated by theoretical chemists, is just now starting to emerge as a viable form of chemical catalysis.[2] This form of catalysis arises because formally covalent species can be stabilized via charge-separated resonance contributors. A non-polar covalent bond A–B might be written as [A–B ↔ A^+–B^- ↔ A^-–B^+], but in the absence of an electrostatic force A–B is dominant and the extent of resonance is small. The presence of an appropriately-oriented electric field can enhance the stability of ionic structures thereby increasing the resonance stabilization of the bond, and accordingly its polarity and hence electrostatic stabilization. Such electrostatic effects can influence the reaction energies and also the barrier heights, depending on the valence bond (VB) contributors involved and the orientation of the field. The Companion Tutorial outlines

[a] *Department of Chemistry, Curtin University, Bentley, Western Australia 6102, Australia.*
[b] *ARC Centre of Excellence for Electromaterials Science, Research School of Chemistry, Australian National University, Canberra, Australian Capital Territory 2601, Australia.*
[c] *Department of Chemistry, Faculty of Natural & Mathematical Sciences, King's College London, Britannia House, 7 Trinity Street, London SE1 1DB, United Kingdom.*
† These authors contributed equally to this work
Electronic Supplementary Information (ESI) available: [details of any supplementary information available should be included here]. See DOI: 10.1039/x0xx00000x

this theory in detail and provides guidelines for predicting and maximizing these effects.

While electrostatic catalysis is a relatively new concept in synthetic chemistry, it is a cornerstone of biological catalysis, where it occurs naturally by binding the substrate in an optimal position relative to charged functional groups in a protein. Arieh Warshel was one of the first to propose the concept of an electrostatic contribution to catalysis.[3] Starting from the 1970s he suggested that the polarity of active pockets had been an overlooked aspect of enzymatic reactions. This idea was finally supported experimentally in 2014, when Boxer and co-workers demonstrated a link between charge anisotropy in enzymes and chemical catalysis.[4] For an ensemble of enzymes embedded in a polymer or vitreous matrix, vibrational Stark effect spectroscopy provides a window on the magnitude of the local electric field (LEF) in the active site. For ketosteroid isomerase, one of the fastest enzymes known, as well as for more recent examples of other complex biomolecules,[5] they demonstrated that the active-site electric field is significant, thus helping to support the idea that electrostatic effects assist in the stabilization of transition states.

However, for catalysis in synthetic chemistry the obvious challenge is how to align molecules and field, so as to take advantage of this field-induced stabilization of ionic structures (Figure 1). We and others have recently demonstrated the first experimental links between directional electrostatic fields and reaction kinetics and thermodynamics. We have achieved this using designed local electric fields (D-LEFs) from charged functional groups,[6-8] using oriented-external electric fields (OEEFs) on single-molecule reactions in scanning tunnelling microscopy (STM) experiments,[9, 10] and using interfacial electric fields (IEFs) in a range of electrochemical techniques to probe the effect of the double layer on both redox and non-redox reactions.[11-14] All of these recent works provide experimental proof-of-concept of electrostatic catalysis on specific sets of chemical reactions, and overturn the long-held assumption that static electricity can only affect rates and equilibrium position of redox reactions. Most importantly, they also provide glimpses of the wide-ranging potential of external electric fields for controlling chemical reactivity and selectivity.

Despite the existing knowledge base in biocatalysis, and despite recent nanotech examples for the organic synthesis of small molecules,[9, 15] the prospect of this form of catalysis entering mainstream "bench" chemistry requires parallel developments on two fronts: i) demonstrating the role of electrostatic effects using problems across different sub-fields of chemistry and ii) a conceptual path to a scalable technology. This will shape our practical understanding of electrostatic catalysis and will bring this new knowledge into the realm of chemical methods that are both clean and able to process workable quantities of materials. The purpose of this tutorial review is therefore to outline methods for harnessing electrostatic catalysis, and to illustrate them with key practical examples. Moving from the nano to the macro-scale, we first outline the use of OEEFs in electrified STM gaps using low dielectric solvents, we then discuss the use of the IEFs in a range of electrochemical techniques to study electrostatic effects on redox and non-redox reactions, and we conclude the use of D-LEFs from charged functional groups to provide a truly scalable source of electrostatic catalysis.

2. Single-molecule reactions in a Scanning Tunnelling Microscope (OEEFs)

Traditionally chemical reactions have been studied using common analytical techniques such as NMR, mass spectrometry and UV-Vis spectroscopy. These bulk analytical techniques measure simultaneously millions of molecules randomly oriented in solution. While powerful for studying macroscopic properties, they limit our understanding of individual reaction pathways that might be washed out by averaging data from billions of molecules. The quest to study chemical reactions at the single-molecule level was eventually realized by the Nobel prize–winning invention of Binnig and Rohrer in the early 1980s,[16] the scanning tunnelling microscope (STM), which has since been a celebrated tool for surface scientists owing to its high precision in atomic scale imaging.

In a typical STM experiment, an atomically sharp metallic tip is scanned along a conductive surface, usually without making physical contact with it. Upon applying a bias voltage between the surface and the tip a tunnelling current is detected when the two electrodes are in nanometre proximity from each other. The tunnelling current is then used to construct an image of the surface with atomic-scale precision.

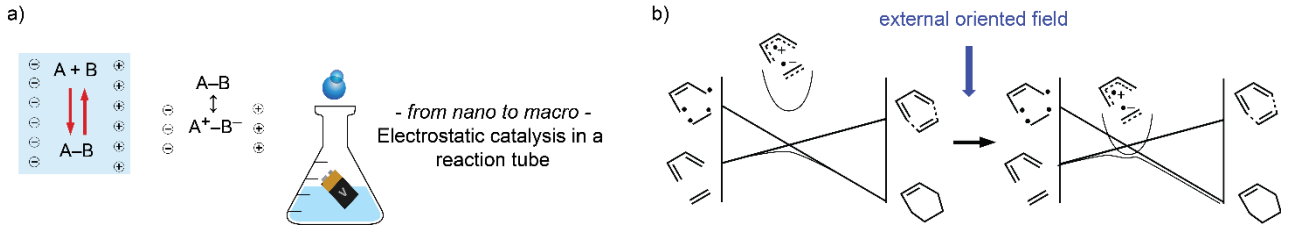

Figure 1. Accounting for electrostatic effects on chemical bonding. Electrostatic catalysis is rationalized as the external oriented electric field stabilizing otherwise unfavourable charge-transfer configurations in the transition state. (a) Non-redox catalysis by external electric field-dipoles interactions. This form of catalysis arises because formally covalent species can be stabilized via charge-separated resonance contributors. A non-polar covalent bond A–B might be written as [A–B ↔ A^+–B^- ↔ A^-–B^+], but in the absence of an electrostatic force A–B is dominant and the extent of resonance is small. The presence of an appropriately-oriented electric field can enhance the stability of ionic structures and dramatically lower reaction barriers. (b) The Diels-Alder reaction, a classic example of a non-polar and non-redox bond-forming organic reaction, is catalysed by an electric field,[9] with the additional possibility of the field affecting endo-/exo-selectivity.[17] We have experimentally shown that an external electric field oriented along the "reaction axis", leads to catalysis.[9]

Traditionally considered to be an imaging apparatus for physicists, over the last decade STM has developed further to become a chemist`s tool to study unimolecular reactions at the single-molecule level by controlling the electric field between the tip-sample junction and the tunnelling current. Initial approaches to study chemical reactivity in STM has typically involved the immobilization of highly reactive molecules at metal surfaces while monitoring changes in their appearance as a response to an external stimulus such as light or heat. Classic examples of these experiments include studies of the photo-isomerization reactions of photochromic dyes,[18] the dissociation of C_6H_5I,[19, 20] and the thermally activated cyclization of ethynyl benzene derivatives.[21] In such cases high resolution STM images, usually at cryogenic and ultra-high vacuum conditions,[20] have been used to accurately follow bond-breaking/forming by creating images of atomic resolution of the reactants and the products.

2.1 Electric field- and electron tunnelling-induced reactions in STM

While early studies of single molecule reactivity involved the study of reactions triggered by light or heat, STM can itself be used to trigger chemical reactions without external forces via two quite different mechanisms: electron tunnelling excitations (vibrational or electronic) or by electric field effects. In the former, the reaction yields depend on the tunnelling current while the latter is operative even in the absence of tunnelling of electrons. The two mechanisms have been differentiated in several studies but are occasionally used simultaneously to explain bond-formation or breakage. This especially applies to the cases where the STM electrodes are in close enough proximity to allow tunnelling of electrons. Below we give a brief description of the e-tunnelling effects, and then focus on the electric field effects and on ways to differentiate between the two mechanisms.

2.1.1 e-Tunnelling-induced reactions. When an electron tunnels through a molecule, inelastic electron scattering can induce vibrational excitations in the molecule resulting in energy transfer from the electrons to the bonds of the molecule. When the tunnelling electron loses energy matching or exceeding the bond energy, bond breaking can occur. Alternatively excitation of the electron to an upper electronic state via a Franck-Condon transition can occur, which may lead directly to bond-breaking, or serve as a state that leads to vibrational excitation upon return to the ground electronic state.[22] Experimentally, to break a bond, the STM tip is positioned above the location of the bond of interest and then the tunnelling electrons are injected by voltage pulses to induce bond rupture. This mechanism has been frequently used to explain STM induced bond-breaking. Examples include the dissociation of single iodobenzene molecules[19] and C–H bond dissociation of trans-2-butene to give 1,3-butadiene.[23] Other e-tunnelling induced reactions includes hydrogen tautomerization of melamine and napthocyanine derivatives.[24, 25]

2.1.2 Electric field-induced reactions. Another “invisible” stimulus that can induce a chemical reaction is the electric field that is necessarily present at an STM junction, with or without tunnelling of electrons. Hence care should be taken to dissect electron tunnelling from electric field effects in STM chemical reactions. Electric field effects that induce STM chemical reactions have been observed experimentally in the absence of any tunnelling current.[10, 26, 27] These reactions were often explained by the ability of the electric field to distort the transition state potential and lower the reaction barriers. Reported examples include the cis-trans isomerization of azobenzene and ring-closure of diarylethene molecules in STM experiments.[10, 26, 27] Electric field effects have also been suggested to play a role in triggering desulfurization of tetracenothiophene,[15] the reaction between Fe and CO molecules to form $Fe(CO)_2$ complexes,[28] and methanol oxidation.[29]

2.1.3 Tunnelling versus electric field effects. Grill and co-workers have conducted elegant experiments to dissect electric field effects from electron tunnelling effects.[26] The group used voltage pulses to isomerize azobenzenes between its cis and trans isomers. To eliminate any tunnelling current, the authors separated the two STM electrodes at a distance at which tunnelling of electrons cannot occur. This was possible as current decays exponentially with distance in STM. The relationship between the applied bias voltage necessary for switching and the tip height was used to show that the process is caused by the electric field and not the tunnelling of electrons. These studies also showed that bias polarity has an effect on the efficiency of switching azobenzenes, an effect that can only be related to electric field since the bias polarity should not change the magnitude of the tunnelling current. Similar directionality effects have been observed in our STM reactions that are described below (Section 2.2) that also points towards electric field effects as the cause of catalysis.

2.2 Tools to quantify the effect of electric field on chemical reactions

The early studies of field effects on reactions in STM experiments, as outlined above, focussed on unimolecular processes. To measure and harness oriented external electric fields (OEEFs) for catalysis of bimolecular reactions entails several technical challenges. This is because (i) relatively high field strengths are needed (ii) only very large datasets can provide a quantitative understanding, and most importantly of all (iii) the orientation of the approaching reactants has to be precisely controlled, even when adsorbed on a surface. To join the two reactants and to form a bond between them they have to be in close proximity to each other and their reaction axis must align properly with the electric field. To this end, we utilized STM and surface chemistry techniques, in which one reagent is tethered to the surface of an STM tip and the other to the STM substrate. In this way their orientation in the field is controlled. The potential difference between the tip and the

substrate can be precisely adjusted through the STM bias voltage. This will dictate the charge density on the small metal tip, hence the field just outside it. The reaction rate is then measured as a function of the bias voltage and direction, using one of the following two methods.

2.2.1 The "Blinking" method. One of the effective approaches to monitor a chemical reaction at the single molecule level is the blinking approach, which we adopted from the pioneering current-time method of Nichols and co-workers.[30] The method allows transient formation of a molecular wire through sudden jumps or blinks in the monitored tunnelling current (Figure 2a). We exploited this methodology to detect the formation of product molecules through the measured tunnelling current as a consequence of either closing or opening the tunnelling gap between the two electrodes. When two reactants (A and B) are joined in a bimolecular reaction (A + B → A–B), the product molecule spans the gap between the electrodes and closes the electrical circuit (Figure 2a, step 2). This leads to an increase in the current above the background tunnelling current (tunnelling through the gap space, steps 1 and 3) and is reflected in the sudden jumps in the monitored current in the form of telegraphic signatures or "blinks".[9] The current then drops back to the through-space tunnelling current after the bond between product molecule and tip (or substrate) is broken as the tip is moved in the x-y directions (Figure 2a, step 3). Hence by holding the STM tip at a fixed z-direction distance from the surface and scanning in the x-y directions at a fixed rate, A–B chemical reactions can be counted per unit time.

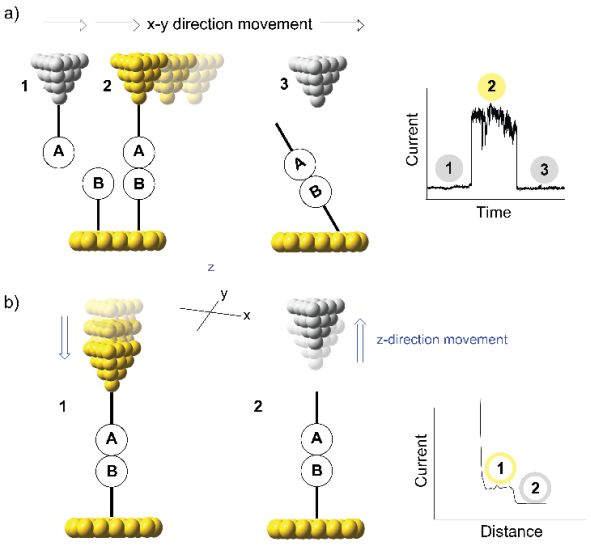

Figure 2. Schematic depiction of STM junction experiments used to study OEEF effects on bimolecular reactions. a) Depiction of the blinking method in which the STM tip and the substrate are functionalized with molecules of interest; the two electrodes are then brought in close contact and the z-height is fixed; the tip is then scanned in the x-y direction. Single-molecule reactions are detected via sudden jumps "blinks" in the monitored tunnelling current. b) Tapping method where the STM tip that is modified with one reactant is pushed in and out of contact along the z direction to/from a substrate functionalized with the other reactant. When the STM tip is pulled away, plateaus appear in the current versus distance profile, which are attributed to the stretching and breakage of the product molecules formed.

2.2.2 The "Tapping" method. This method is based on the STM-break junction method of Tao and co-workers where an STM tip is modified with one reactant (A) and pushed in and out of contact (z-direction) to/from another electrode functionalized with reactant (B).[31] During the contact, chemical reactions between A and B can close the circuit and increase electron tunnelling above the background rate (Figure 2b, step 1). When the STM tip is pulled away, plateaus appear in the current versus distance profile, which are attributed to the breakage of the product molecule occurring from its weakest point, usually the contact between the molecule and the tip or substrate of the STM (Figure 2b, step 2). This process can be repeated thousands of times so that the yield of single-molecule reactions can be determined from the number of molecular junctions formed divided by the total number of collisions attempted. Because the z-distance between the two STM electrodes can be rapidly manipulated, the tapping method can also be used to detect the formation of products (e.g. in probing reactions where the products have different dimensions to that of the reactants).

2.3 Bond forming experiments

In 2016 we demonstrated a first proof-of-concept for 'electrostatic catalysis' by exploring these field effects on an unfavourable Diels-Alder coupling process.[9] We used the STM Blinking method and selected a Diels-Alder reaction for our case study so as to test Shaik's pioneering predictions of electrostatic catalysis for this reaction class.[17] We chose reagents that were relatively unreactive and non-polar to provide a clear test of whether electrostatic effects were important. A gold STM tip was modified by attachment of a diene molecule, and a gold substrate was modified with a relatively rigid dienophile (Figure 3a). When a voltage (bias) is applied between the STM tip and the substrate and they approach at a tunnelling distance (ca. 1nm), high electrical fields (up to several V/nm) are generated. These are oriented along the main tunnelling junction axis, and can accelerate the Diels-Alder reaction. The blinking method was used to quantify the rate of product molecular formation through the frequency of "blinks', i.e. the formation of product molecules, from the monitored current flowing through the tunnelling junction (Figure 3b).

Quantum-chemical modelling of the system predicted that at these field strengths only an electric field pointing from the diene to the dienophile would increase the reaction rate, in turn due to its ability to stabilize the dominant ionic resonant contributor (Figure 4a). Over the same range of field strengths, the reaction rate was predicted to be independent of field strength. Experimentally we showed that, indeed, for positive bias there is a measurable reaction rate that is independent of field strength, up to the limits of the experiment, while for negative bias the rate increased by up to a factor of 5 over the same range (Figure 4b), consistent with the quantum-chemical predictions.[9]

2.4 Bond breaking experiments

Unlike bond-forming, bond-breaking does not require the same level of fine-tuning of the distance between the two electrodes. Here, the tapping method is more suitable as its rapid z-direction manipulation allows detection of products that have different dimensions to those of the reactants. In this way, thousands of distance-current curves can be generated in a short time, enabling access to a statistically significant pool of data on the probability of bond breaking as a function of changes in field magnitude.

We have explored the role of electric fields on the lysis of alkoxyamines (C–O bond breaking) by bridging an alkoxyamine molecule (Figure 5) between a gold STM tip and gold substrate under a bias stimulus of variable magnitude.[11] At low biases we observed the exclusive presence of the parent alkoxyamine molecule. Between 100 and 200 mV, however, a mixture of nitroxide species and the parent alkoxyamine are present. Above 200 mV, the only species detected are the nitroxide radicals. Nitroxides have a known affinity for gold surfaces and the same conductivity signature is observed in control experiments that are performed using a standard nitroxide (4-amino-TEMPO) solution confirming that nitroxide radicals are indeed the product of an OEEF catalysed (C–O) bond breaking of alkoxyamines. The role of the electric field in promoting the homolysis of the alkoxyamine has been explained by quantum-chemical calculations of the reaction profile in the presence of an electric field of varying strength that is aligned along the N–O bond axis. These calculations suggest that the homolysis of alkoxyamines can be promoted by as much as 35 kJ mol^{-1}. This barrier lowering effect is consistent with the expected stabilization of the charge-separated resonance contributor to the nitroxide radical (N–O$^{\bullet}$ ↔ N$^{+\bullet}$–O^{-}) and is enough to account for the radical formation.

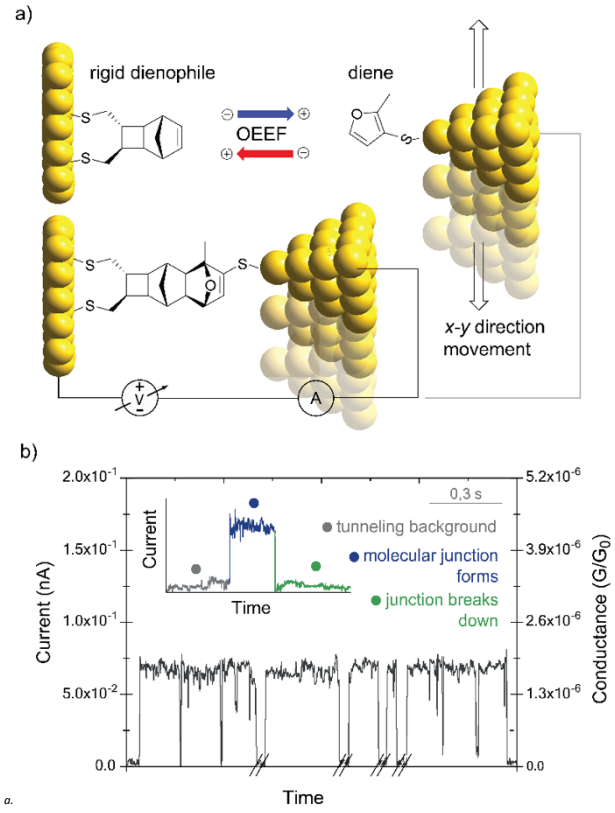

Figure 3. Single molecule reaction studies in STM under an OEEF. (a) The field effect on the reaction rate is studied using the STM blinking approach. A furan is attached to the STM tip via a thiol group. A norbornylogous bridge, the dienophile, is attached in a known orientation to a flat gold surface via two thiols. The rigid norbornylogous bridge enables exposing the alkene moiety at the monolayer distal end.[9] (b) Typical results obtained showing plateaus formed in the current versus time trace due to reaction-induced junction formation. Junctions are subsequently broken as the tip continues to scan.

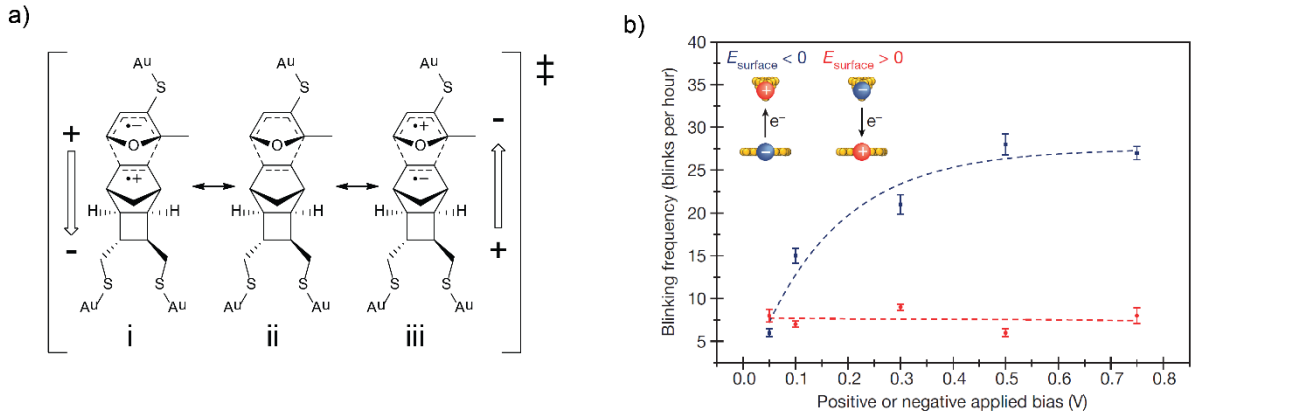

Figure 4. A single-molecule Diels-Alder reaction under an OEEF; origin and magnitude of the effect.[9] a) The possible resonance structures of the transition state of the Diels-Alder reaction studied in Figure 3. In the presence of an electric field, minor contributors I or III may be stabilized enough to undergo resonance with II, lowering the reaction barrier, with I being the most feasible configuration. The vertical arrows show the field direction most likely to stabilize I or III, with I expected to experience greater stabilization at a given field magnitude. b) Changes to the frequency of blinks as a function of the applied bias. Blinks reflect the formation of products detected when the tip and substrate were separated by a distance that allows the Diels–Alder reaction to occur (about 1 nm). Junctions were formed only when both reactants were present. For positive bias there was a measurable reaction rate that was independent of field strength up to the limits of the experiment, while for negative bias the rate increased by up to a factor of 5 over the same range. Part (b) is adapted with permission from Ref. 9.

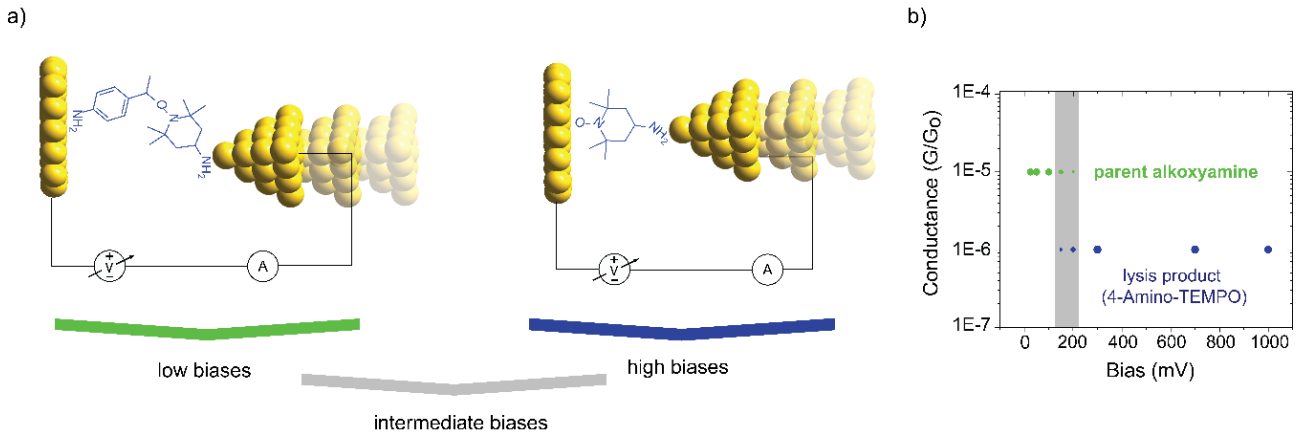

Figure 5. An EEF prompts the lysis of alkoxyamines; C–O bond breaking under an electric field. Schematics of a scanning-tunnelling microscopy single-molecule tapping junction experiment on alkoxyamines in low dielectric solvents. (a) The fate of the parent alkoxyamine (left panel) is probed by measuring the single-molecule conductivity at different field strengths. The bias is from substrate to tip, but the relative orientation of the molecules is not controlled. Molecules have very distinct electrical finger-prints in STM junctions and for instance the 4-amino TEMPO molecule (lysis product in the right panel) is less electrically conducting than the parent alkoxyamine by one order of magnitude (ca. 1×10^{-5} and 1×10^{-5} of G_0, ($G_0 = 2e^2/h$ = 77.5 μS, quantum of conductance). (b) From the analysis of several thousands of single-molecule experiments (ca. 4000 at each bias) it is apparent that the STM tip-to-substrate bias guides the redistribution between an alkoxyamine-only population (up to ca 100 mV of dc bias between STM tip and substrate) to a mixed alkoxyamine/nitroxide population (between 150 and 200 mV) and ultimately to a nitroxide-only presence (biases over 300 mV).[11]

3. Harnessing IEFs in Electrochemical cells

As discussed in the previous section, STM-tapping and-blinking allows collection of a statistically-significant amount of experimental data in short time frames. It can be used in pure liquids and at room temperature to simultaneously orient tethered reagents in a tuneable electric field and measure how the field affects the rate of reaction.[9, 11, 32-34] These types of electrical measurements are arguably the gold-standard to guide the trajectory of approaching reactants and to study chemical reactions at the single-molecule level under a precise electric field. They enable the rapid screening of reactions under an accurate control of field magnitude and direction, and have already been applied successfully to isomerizations,[33] bimolecular bond-forming,[9] and bond breaking processes.[11, 15] These experiments are however unlikely to be of practical value towards bulk chemical synthesis. To provide a scalable method for harnessing external electric field effects, a different approach is required and for that we initially turned to the electrochemical cells normally used for faradaic reactions.

A description of the origin and practical implications of the capacitive nature of a solid/liquid interface in electrochemistry, surface, and colloid science is included in the Supporting Information. Below we seek to summarize the often-overlooked electrostatic effects of the electrical double layer on redox reactions, and non-redox reactions. In the latter case we will examine what is the potential scope of electrostatic catalysis in diffusive and diffusion-less systems, and discuss platforms to take the study of single-molecules to a molecular layer and eventually to a completely scalable diffusive platform for electrostatic catalysis at a macroscopic electrode/electrolyte interface.

3.1 Near-surface electric fields at electrode/electrolyte interfaces

Bulk electro-neutrality is lost near an electrified interface;[1] and the assumption of electro-neutrality, true in bulk solution, is no longer valid near the interface. Surface potentials drop with increasing distance from the electrode by a factor 1/*e* (*e* being the Euler's number) for each successive Debye length (see Textbox 1). By using an ideal reference electrode any change to the potential difference between the reference and working electrode will translate exactly into the same potential difference change between the working electrode and bulk electrolyte solution. As the potential is changed, ions in solution move without being either oxidised or reduced, and in fact the potentiostat records a measurable current even in the absence of electrolysis (i.e. no net chemical change). In other words, charges on the electrode that establish a potential difference with respect to the bulk solution need to be compensated by an excess of ions of the opposite charge, something akin to a double layer of charges (Figure 6a).

Salting-out of colloidal particles is a classic textbook example that is often used to illustrate this otherwise abstract concept of a double layer. Ions around the surface are subject to thermal diffusion and hydrodynamic drag creating a “cloud” of counter-ions above the surface known as the electrical double layer, or Debye layer. The salting-out occurs when the “reach” of electrostatic forces is short and so the colloidal particles have a greater chance of colliding against

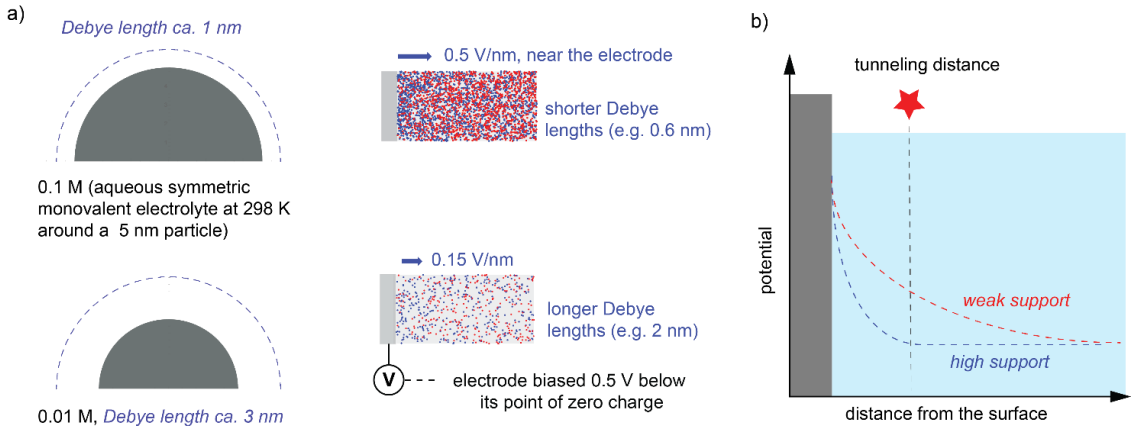

Figure 6. A charged surface immersed in an electrolyte solution attracts ions of opposite charge, effectively screening the charge on the surface. The charge in the electrical double layer or Debye layer is equal and opposite of the charge on the surface. (a) The Debye length indicates the depth of the "cloud" and is an important parameter in colloid science. The reach of electrode charges is shorter in highly-supported electrolytes so that this double layer is narrower (i.e. larger V/distance numbers) for the more conductive solution (here 0.1 M versus 0.01 M, *i.e.* high versus low electrolytic support). The distribution of chloride (red symbols) and sodium ions (blue symbols) around a flat electrode/electrolyte interface where the potential in the bulk solution (ϕ_s) is 550 mV more positive than the potential at the electrode (ϕ_M) is schematically shown. The Debye length is independent of the potential difference, and the near surface V/nm figure can be as high as *ca*. 0.5 V/nm for a 0.25 M NaCl aqueous electrolyte (upper panel), or as low as 0.15 V/nm for a 0.025 M solution (lower panel). The existence of a double layer of charges at an electrode/electrolyte interface is also indirectly manifested in electrode kinetics and thermodynamics. Applying a charge to an electrode will cause an ion to be attracted or repelled by that charge. (b) In electrode kinetics the full potential difference applied between the working and reference electrodes is 'sensed' only by molecules that approach the interface in highly-supported electrolytes.

Textbox 1.

Electrical Double layer. The electrode surface holds a charge density which arises either from an excess or deficiency of electrons. Charges on an electrode establish a potential difference with respect to the bulk solution need to be compensated by an excess of ions of the opposite charge. This leads to two layers of charge and hence the term double layer. For more information on the models used to describe the ionic environment near a surface see S1 of the ESI.

Debye Length. The Debye length in the context of a charged surface in an electrolyte is a characteristic distance at which significant charge separation can occur in the electrical double layer. The Debye length is proportional to the reciprocal of the ionic strength. The higher the ionic strength, the more shielding of the charged surface, and the thinner the Debye length.

Space-Charge Layer (SCL). Inside an electrolyte, anions and cations carry the charge. Inside semiconductors this is done by holes and electrons. However, near the surface, electrons and holes are not found in equal numbers, implying that there is a potential decay (i.e. a field) inside the semiconductor. This excess of charge density decays to zero inside the solid and the thickness of this electronic cloud, the space-charge layer (sometimes indicated as space-charge region), drops as the bulk concentration of charge carriers increases, just as the double layer gets compressed when the electrolyte concentration is large.

each other, thereby coagulating and dropping out of solution. According to classic electrolyte theories, within the dilute (Debye–Hückel) regime, the screening length decreases with increasing concentration of the electrolyte (Figure 6a). The Debye length scales inversely with the square root of bulk ion density, at least up to modest concentrations of salts (~0.1 M).[35] In other words, the electric field extends further into solution for lower conductivity electrolytes (i.e., under conditions of weak support, Figure 6b).

In addition to affecting the stability of colloids, electrostatic forces in a double layer manifest in many other forms including inducing the physical movement of molecules towards and away from an electrode (voltage-responsive self-assembled monolayers in Figure 7)[36]; exerting subtle effects on the apparent formal potential of redox probes that are precisely localized within the electrical double layer[37]; stabilizing ionic structures of reaction intermediates and hence guiding the selectivity of chemical reactions by field–dipole effect[13, 14]; and ultimately promoting non-redox catalysis in both diffusive and diffusion-less, i.e. surface-tethered, systems.

Shifts in apparent formal potential can be used to map the potential profile of the electrical double layer (Figure 8).[37, 38]. Control experiments in Figure 8a show that measurements of

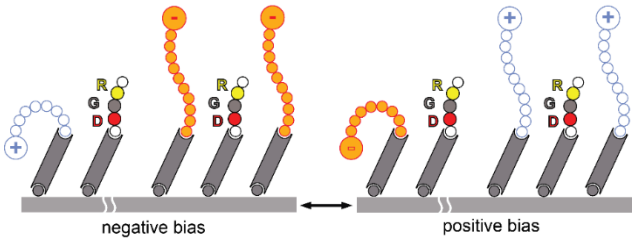

Figure 7. The near-surface field of an electrified silicon electrode is not completely screened in electrolytes and can actuate the reversible migration of charged molecules. Ionic head groups appended to flexible self-assembled monolayers move in response to a voltage switch (+300 or −300 mV vs reference) in order to make accessible or inaccessible to eukaryotic cells the short rigid molecules that are terminated by RGD peptides to promote adhesion and survival of the cell.[37]

redox thermodynamics are linked to the steepness of the Debye layer and not to the distance of the ferrocene probe from the electrified metal. It follows that using a suite of available monolayer chemistries,[39] the experimentalist should be able not just to alter the charge density of the electrode by adjusting voltages,[14] but also to i) gain control on alignment of field vs. reaction axis and ii) doing fine adjustments to the electrostatic stimulus by means of precisely localizing the reaction site, and not necessarily a redox reaction, within the electric double-layer.

3.2 Surface tethered versus diffusive conditions

Electrostatic catalysis is strongly directional, and so an important consideration when moving from STM experiments to electrochemical cells is how should the alignment of molecules be managed. A distinction is made between surface-tethered systems where alignment is better controlled, but cost and scale are somewhat sacrificed, and diffusive systems where there are no external controls over alignment. Our experiments to date suggest that catalysis is possible under both scenarios (see Section 3.3 below). In the case of the diffusive systems, this can be understood in the relative rates of diffusion in the double layer versus reaction. As shown above in Figure 6a, the distribution of chloride and sodium ions for a 0.25 M aqueous electrolyte could possibly lead to a Debye length of 0.6 nm. If the potential in bulk is fixed at 550 mV above or below the potential of zero charge of the electrode, this can potentially translate a voltage/distance drop of ca. 0.5 V/nm in the neighbourhood of the surface. The time scale required for diffusive reactants to travel across this electrified layer is long (~50 μm/s) compared with the time scale of the chemical reaction, confirming that self-alignment in the electric field is possible in principle. As a result, the molecules spend enough time in the double layer to sample many conformations so that if and when an optimal (i.e. reactive) one is sampled, it can be kinetically trapped by the electrostatically catalysed reaction.
This in turn brings a further fundamental question: what is a better effector of chemical change? Is it a steeper voltage drop in the Debye layer (i.e. high support) or a "poorer screen" of the excess surface charges on the electrode (i.e. low support)? Our initial work has identified two scenarios. Diffusive systems are

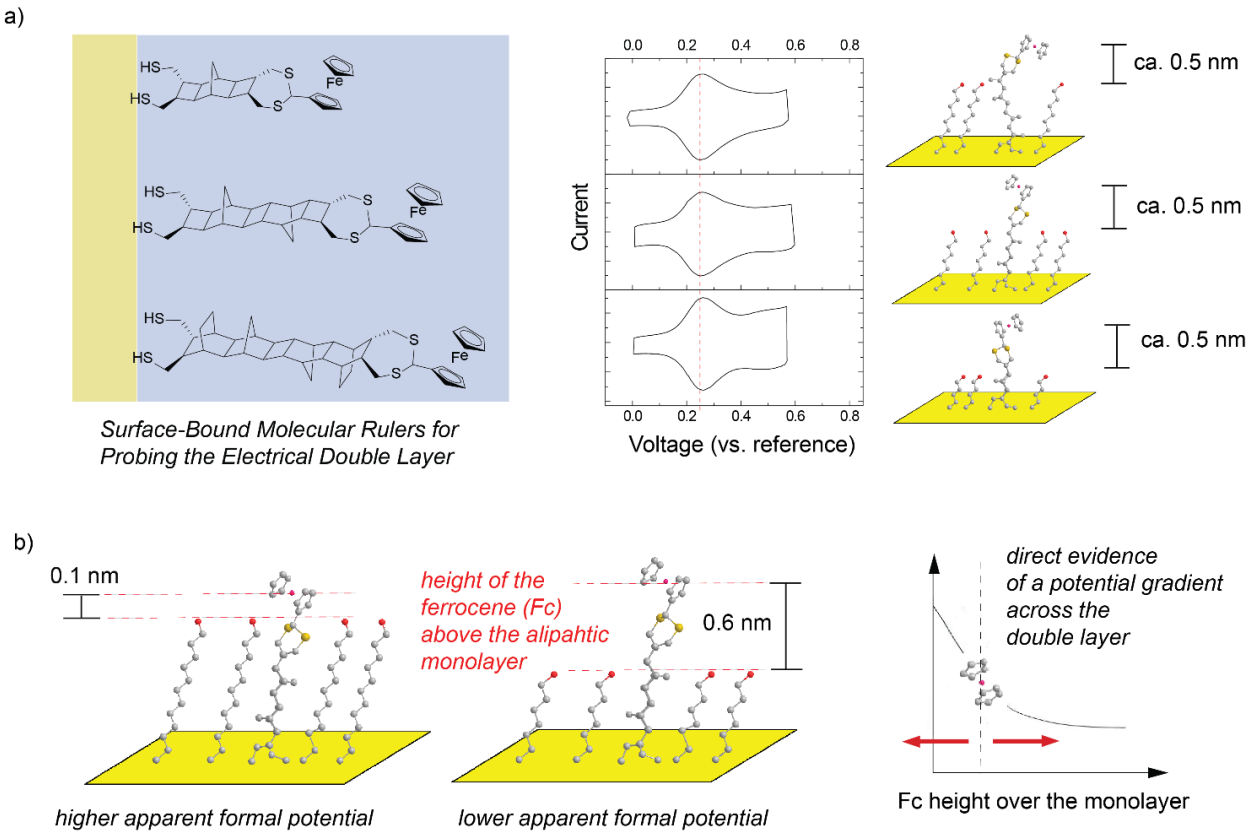

Figure 8. Direct measurement of the potential profile across a metal/electrolyte diffuse layer by using rigid molecular "rulers".[40] Norbornylogous bridges can be used to either change (b) or keep constant (a) the distances between redox centres[38, 40] and the surface plane defined by a monolayer of inert hydrocarbon diluent molecules. These constructs allow fine measurements of the changes to the apparent formal potential to gain insights on the field decay into the bulk solution. The key to achieving this is the rigidity of a norbornylogous bridge; it sits at a well-defined orientation to the electrode surface and unlike flexible molecules it does not change orientation during the redox reaction. This property enables the surface molecule to act as molecular ruler that can position the centre of the ferrocene moiety at precise locations above the electrode with ca. 0.1 nm increments in the distance away from a surface plane defined by the diluent molecules. Hence, the ferrocene moiety acts as a probe which senses the potential gradient by measuring changes to the formal potential while it is progressively moved across the electrical double layer. Only one *trans* diastereomer of each system is depicted in the diagram. The other trans diastereomer has the same geometrical properties with regards to the distance and the orientation of the ferrocene moiety with respect to the surface.

likely to respond more efficiently to shorter Debye lengths, while in surface-tethered systems, and at least presently for the case of semiconductor electrodes, the effect will be larger in a low supported electrolyte.

3.3 Electrostatic catalysis by IEFs: Alkoxyamine cleavage

To examine whether the IEFs in electrochemical cells can provide a practical and scalable platform for electrostatic catalysis, we studied alkoxyamine bond cleavage at room temperature in both surface tethered and diffusive systems (Figure 9).[9] Alkoxyamines are heat-labile precursors widely used as a source of nitroxides in polymer and materials sciences but traditionally require high temperatures (80-120°C) for this purpose. Producing a controllable source of nitroxides at lower temperatures would greatly increase their scope in chemical synthesis. In section 2 of this review (above) we showed that this could be achieved electrostatically by altering the stability of charge-separated contributors (N–O$^{\bullet}$ ↔ N$^{+\bullet}$–O^{-}) using STM tapping experiments.[9] To test whether the same electrostatic catalysis could be performed in an electrical cell, we performed cyclic voltammetry experiments on both surface tethered and non-surface tethered alkoxyamines (Figure 9).

Interestingly both sets of experiments led to room temperature cleavage to product nitroxide radicals, but not in the manner anticipated.[9] Under cathodic polarization we measured no detectable cleavage, but with an anodic wave the alkoxyamine underwent oxidation to a radical cation intermediately prior to rapid irreversible mesolysis to a carbocation and a nitroxide radical. The latter was then further oxidised (reversibly) to an oxoammonium cation, with the nitroxide radical recovered upon subsequent reduction. Based on digital simulations of experimental voltammetry (solid symbols in Figure 9a) and current-time transients,[11] it is clear that the unimolecular decomposition that yields the "unmasked" nitroxide (TEMPO) is exceedingly rapid and irreversible. Together with quantum chemical data and EPR detection of nitroxide radicals also support a stepwise electrochemical-chemical-electrochemical mechanism ($EC_{irrev}E$, Figure 9 and Figure S1 of the ESI) in which the alkoxyamine oxidises (E), then undergoes rapid and irreversible cleavage (C_{irrev}), and the nitroxide radical produced in the cleavage reaction then undergoes oxidation (E).

While this was an electrochemical process, there was nonetheless electrostatic catalysis of the coupled chemical reaction: the mesolysis of the oxidised alkoxyamine to a nitroxide and carbocation. In fact, if the field had been absent, the reaction would have been highly unfavourable (by ca. 35 kJ mol^{-1}) and its rate completely inconsistent with that observed experimentally. In other words, this non-redox reaction is facilitated by the electrostatic environment of the double layer. At the same time, an interfering redox process (alkoxyamine oxidation) prevented the hoped-for homolysis reaction of the neutral alkoxyamine.

Although not useful for nitroxide-mediated radical polymerization, this electrochemical cleavage reaction provides a mild source of carbocations that can be harnessed in orthogonal radical-cationic polymerization processes. Mild sources of carbocations are also of use in small molecule synthesis provided the potential required to generate them is compatible with typical functional groups. The electrochemical cleavage also provides a means of electrically generating persistent nitroxide radicals from alkoxyamines, either on a surface or in diffusive environments, with potential uses in sensing and antioxidant activities.

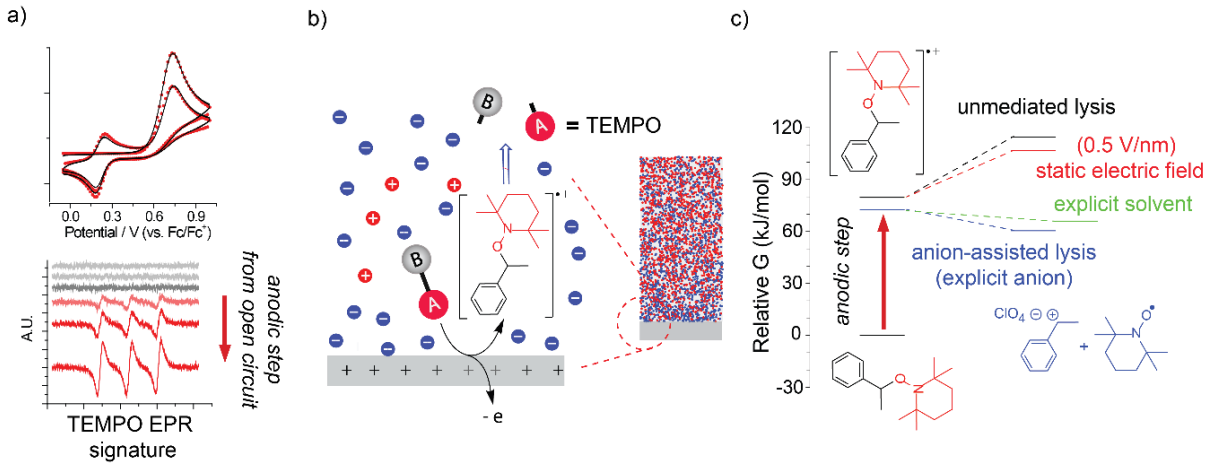

Figure 9. **Anodic chemistry and Debye fields**. (a-b) The fragmentation of an anodized nitroxide is very fast regardless of the anion and the backward reaction is essentially inoperative on the time scale of the experiments. (c) The homolysis of the unperturbed ('free') radical-cation (black pathway) is strongly thermodynamically disfavoured. However, cleavage is made more favourable by a static electric field, by interactions with an explicit anion and/or with an explicit solvent molecule (red, green and blue pathways, respectively). We have experimentally evaluated the role of the anion (ClO_4, PF_6 and $B(C_6H_3(CF_3)_2)_4$) over a wide range of sweep rates, concentrations and solvents and found almost complete ion-insensitivity, supporting an electrostatic basis for the catalysis.

This recent study provides proof of concept for electrostatic catalysis of a non-redox bond breaking reaction under both diffusive and non-diffusive conditions. From a practical perspective it also serves as a warning: that one must consider potential redox processes as competing or complementary reactions in any experimental design. To avoid unwanted redox reactions, one needs to protect or avoid functional groups that easily undergo oxidation or reduction (depending on whether an anodic or cathodic electrode is being used to catalyse the chemical process). At the same time, the study serves to highlight the unappreciated role that electrostatic catalysis may already be playing in, for example, electro-organic chemistry.[41] This is important as chemical and electrochemical methods for oxidation or reduction are usually assumed to be interchangeable. However, only electrochemical methods offer the possibility of electrostatic catalysis of any linked chemical steps. Hence electrochemical methods may open up redox triggered chemical reaction pathways not previously considered, likewise chemical redox methods help to suppress unwanted chemical side reactions that occur under electrochemical conditions.

3.4 IEFs in surface reactions; insulating and semi-conducting surfaces

Another approach to harnessing interfacial electric fields for catalysis is at insulating surfaces. For example, Kanan and co-workers have used elegant surface-chemistry on insulating Al_2O_3 films to study the effect of static charging on carbene reactions and epoxide rearrangements in electrolyte solutions (see also Companion Tutorial).[13, 14] The use of an electrical insulator removes in principle the task of decoupling electrostatic from electrochemical effects. There is however one serious caveat with insulators; they can gain excess surface charging, but in a material that by its own nature does not conduct electricity, and it is hard to define and systematically control and measure these effects. This task is further complicated by surface ionization and adventitious adsorption reactions.

We have therefore begun to explore whether, under the effect of an external bias, it is possible to measure an electrostatic effect on a surface tether when transient faradaic currents are allowed to flow at semiconductors.[12, 39]

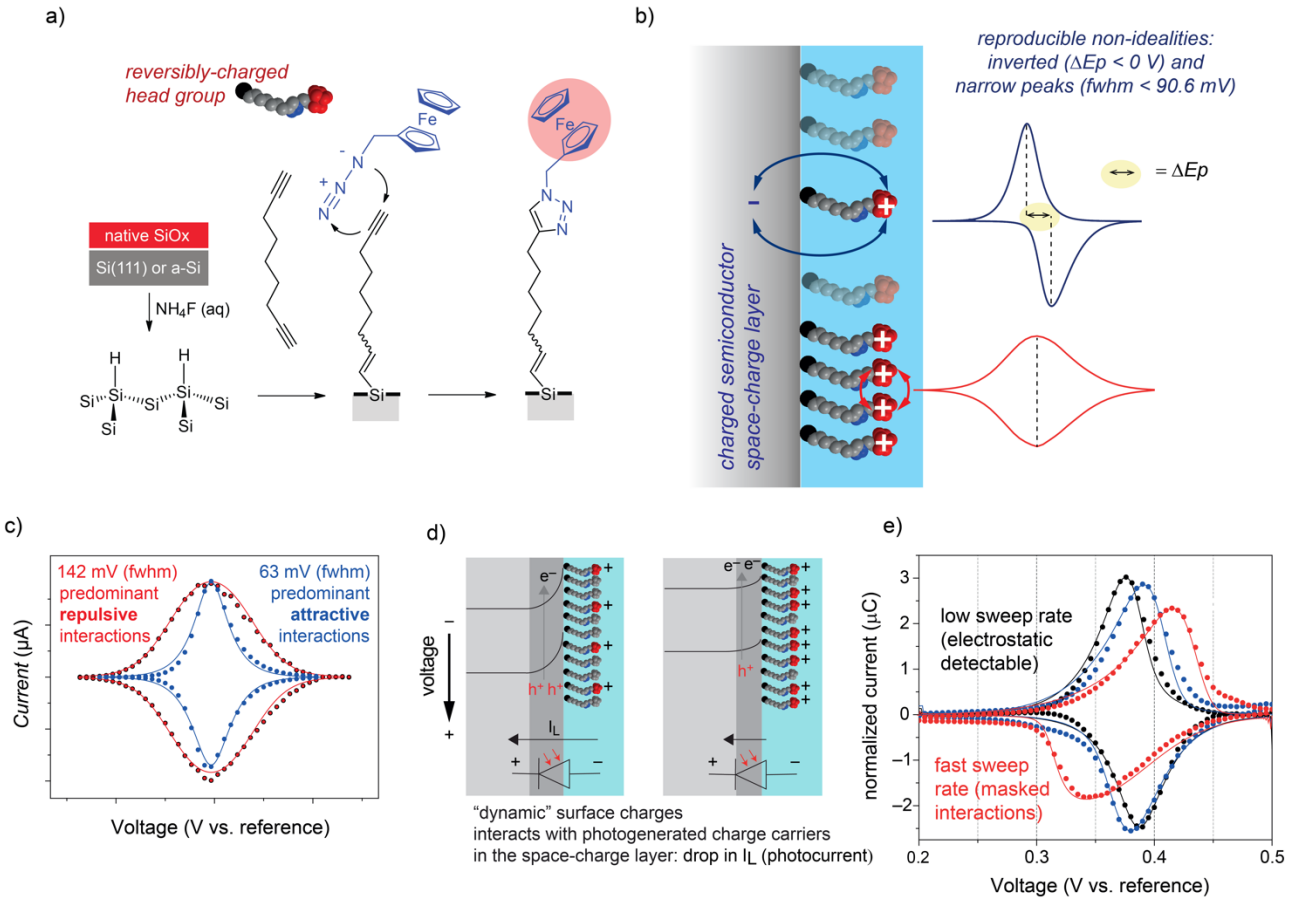

Figure 10. When "flaws" are accounted for: semiconductor space-charge effects on the activity of surface charged molecules.[12] (a-b) Light-assisted hydrosilylation of 1,8-nonadiyne at a Si-H electrode and attachment of azidomethylferrocene to yield redox-active monolayers. (c) Representative background-subtracted voltammograms and simulated traces (solid red line) for "as-prepared" samples (symbols) indicate repulsive forces dominate the electrostatic balance of the monolayer system. Applying a potential step of 0.3 V for 140 s suffice to remove dielectric screening by the carbonaceous film and shifts the balance in favour of attractive interactions (blue line and symbols). (d) Distortion of the semiconductor-side of the barrier from the presence of an electrochemically-induced dipole layer of surface charges. (e) Quantitative model (solid symbols) for near-surface charging effects in electrolyte systems and in the presence of electrochemical currents with peak-position "inversion" becoming apparent at low sweep rates.

In this context we believe that monolayer chemistry (see Figure S2 of the ESI), and especially covalent monolayers at oxide-free silicon electrodes,[42] provide an ideal platform to orient molecules in an electric field so as to take advantage of near-surface electrostatic effects (see Figure S3 of the ESI). By separating electrostatic effects from electrochemical effects, we can also study catalytic cycles that involve for instance a mixed sequence of redox and non-redox steps. A key example is cytochrome P450, where intriguing theoretical predictions by Shaik suggest an oriented external electric field could be used to promote both its non-redox gating and the two reduction steps in the cycle, thus increasing the enzyme's efficiency *at will (see* Figure S4 of the ESI).[43]

The impact of electrostatic effects on semiconductor electrochemistry, often under-appreciated, can be dramatic. The electrostatic landscape of silicon is particularly rich, and the poor Debye screening of this material results in a fraction of the applied bias appearing inside the semiconductor phase itself. As a result, there is a complex interplay between this penetration zone, which is known as the space-charge region (SCL, see Figure 10), the screening of the space-charge region by the electrolyte and the charged layer of surface dipoles. It is known that excess surface charges at the organic monolayer in a vacuum can affect the charge distribution inside the space-charge, and recently we have shown that these static effects also manifest at a solid/liquid electrolyte interface in electrolyte systems and in the presence of electrochemical currents. Contrary to the more common situation of a metal-semiconductor contact,[44] we found localized charges accumulate not at step edges or defect sites but in a redox monolayer immediately outside the semiconductor SCL (Figure 10b).[12]

Interestingly, these electrostatic interactions lead to reproducible electrochemical non-idealities (fwhm's < 90.6 mV and "inverted" peaks, $E_{\text{peak cathodic}} > E_{\text{peak anodic}}$) and non-ideal peak shapes and positions in voltammetry. These features, often rejected as flaws, are actually the manifestation of electrostatic forces between charged redox molecules and the semiconductor's SCL (Figure 10). We have developed an analytical model to decouple, under finite kinetic limits, the electrostatic molecular effects on the semiconductor side of the barrier (i.e. diode effects) from the electrostatic effects among surface-bound molecules (i.e. effects on the Frumkin isotherm). The model explains the interplay between these factors and highlights the impact of molecular charges on the interfacial potential distribution at semiconductor electrodes.

This work has immediate implications for the kinetic analysis of charge-transfer reactions at semiconductors: it reveals the impact of molecular charge effects on the interfacial potential distribution at a semiconductor electrode. Even more importantly, this evidence of a cross-talk between surface molecules and excess charges in the semiconductor space-charge has greatly aided the study of IEFs on chemical reactivity. Any IEF effect in a diffusive system likely to be aided by the charge gradients and ionic aggregates within the Debye layer (Figure 9), bearing in mind that the characteristics of this charged region depend only on the properties of the solution, not on the surface that it screens. Key parameters will therefore be ion concentration, ion valence, relative permittivity, and temperature of the fluid. Based on unpublished preliminary studies of pericyclic reactions, the situation appears to be very different for IEF effects on surface bimolecular reactions (diffusion-less systems). In that case catalysis is only expected be appreciable in low screening systems, that is, at a very low level of electrolytic support, and only for semiconductors operating in accumulation.

3.5 Summary

Electrostatic effects at insulators, semi-conductors and conductors can be large and can be harnessed for catalysis of non-redox reactions.[9, 11-14] They also influence redox reactions in a manner that has not been fully appreciated until now, and can affect the interpretation of cyclic voltammetry experiments.[12] When harnessing the catalytic effects of IEFs at electrified surfaces, the role of coupled or competing redox processes needs to be considered. Nonetheless, these can often be harnessed in their own right to develop new chemical methods, and through combination with electrostatically driven chemical processes, they offer new prospects in organic synthesis.

4. D-LEFs: pH-Switchable electrostatic catalysis

Scanning tunnelling microscopy (STM) and electrochemical cells provide useful methods for aligning an external electric field to catalyse non-redox reactions. However, there are limitations regarding the accessibility of these methods to synthetic organic chemistry. STM experiments are limited to relatively low yielding experiments and are cost prohibitive for bulk synthesis. Applications in electrochemical cells will in all likelihood be limited to unimolecular reactions that are catalysed as they approach and align to the electrode surface. Harnessing electrostatic catalysis in an everyday laboratory setting will continue to remain elusive if we rely solely on these methods. To harness electrostatic catalysis in bulk, solution phase, multi component reactions, which are useful to conventional organic synthesis, we must consider alternatives to external electric fields.

As discussed in the Companion Review electrostatic effects are directional: they are at their most effective when aligned parallel to the bond axis, or the dipole moment of a molecule and display little effect when aligned perpendicularly. It is thus important to control the direction of the electric field, relative to the reaction centre. One way to achieve this in bulk solution is to use the localised electric fields of carefully positioned charged functional groups, attached to the substrate, catalyst or auxiliary of a reaction. These are referred to as designed local electric field effects (D-LEFs) in the Companion Review. The charged group exerts an electric field that is short-range and thus only affects the molecule, complex or supramolecular assembly to which it is attached. By choosing the position and sign of the charged group carefully, the orientation of the field with respect to the reaction centre can be optimized. The charged group could be a quaternary amine, a charged metal

complex, or could be a Brønsted acid or base in an appropriate protonation state. The use of Brønsted acids and bases offers the added advantage of switching the field and hence catalysis "on" or "off" through simple changes to the pH, and hence has been termed in the literature pH-switchable electrostatic catalysis.

4.1 Distonic radical anions

In 2013, we first observed the ability of remote charges to influence chemical reactions in a high-level quantum chemical study of so-called distonic radical anions in the gas phase.[6] In this work we found that remote anionic functional groups were able to stabilise nitroxide radicals and hence lower the bond dissociation energies of their parent alkoxyamines.[6] The effects were of the order of 20 kJ mol^{-1} for charges that were as much as 6 Å from the radical centre. Moreover, they occurred even when there was no covalent bond linkage between the charged group and radical, or when the charged group was replaced by a point charge (i.e. an electric field), thus confirming their electrostatic origin. The stabilization effects were found to be very general, covering a wide range of combinations of charged groups and delocalised radicals. Among other things, the relative radical stabilities of sugar- versus base- centred radicals in model DNA and RNA fragments were shown to vary by around 40 kJ mol^{-1} depending on the protonation state of the phosphates.[6]

Another feature of these distonic radical anions was that the stabilization of the radical by the anion was such that the singly occupied molecular orbital (SOMO) was no longer the highest occupied molecular orbital (HOMO), a phenomenon known as SOMO-HOMO conversion.[6] The physical manifestation of this behaviour is that the radical anion is predicted to undergo preferential oxidation to a diradical species, instead of the closed shell product normally expected. This is illustrated for the case of a nitroxide radical in Figure 11, where it is seen that the radical anion prefers oxidation to a triplet over the closed shell singlet by ca. 0.2 eV.[6] While SOMO-HOMO conversion was a known phenomenon, these were the first examples in which it could be turned "on" or "off" with pH. Interestingly, this pH-switchable orbital conversion only occurred when the charge stabilized the radical. For example, in the same study it was shown that base-centred nucleic acid radical anions, which were strongly stabilized upon deprotonation of the phosphates, underwent SOMO-HOMO conversion, while in the same system, the sugar-centred radical anions, which were weakly destabilized upon deprotonation did not.[6]

Further studies showed that the stabilizing effects of charges on radicals were directional as expected, but asymmetric in the sense that, for example, the stabilization of a given radical by a negative charge was much greater than the corresponding destabilization by a positive charge in the same position.[45] This was a result of polarisation which enhanced the stabilization and muted the destabilizing effects. Importantly, this resulted in meaningful effects in the bond energies because the polarizability of the resonance-stabilized radicals was greater than that of the non-radical parent compounds. It was later

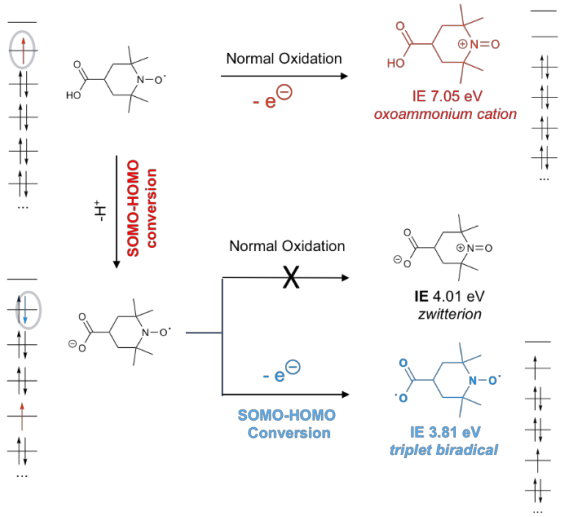

Figure 11. pH switchable SOMO-HOMO conversion of nitroxide radicals. The neutral form follows an aufbau configuration of electrons in which the unpaired electron singly occupies the highested occupied orbital. Upon oxidation the unpaired electron is removed leaving a closed shell zwitterion. The anionic form however undergoes SOMO-HOMO conversion, with the unpaired electron now so stabilized that it no longer occupies the highest occupied orbital. As a result, upon oxidation, a paired electron from the highest occupied orbital is lost, giving rise to a triplet biradical as the preferred oxidation product.

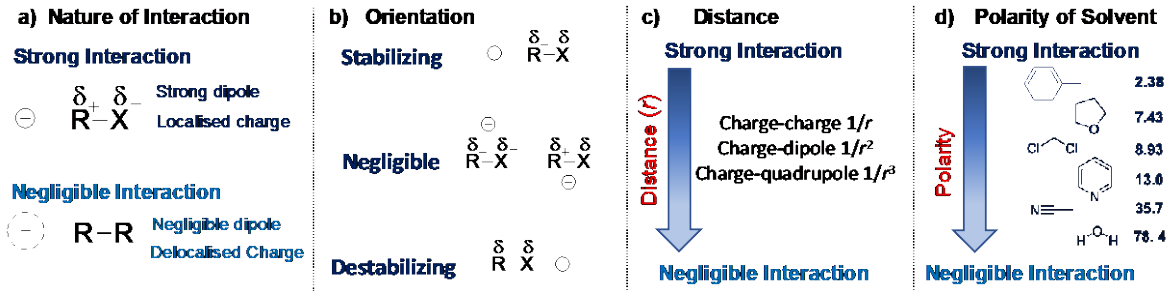

Figure 12. Factors affecting the strength of electrostatic effects on the stability of a species R–X, including a) the nature of the interaction, b) the orientation of the charge respect to the bond dipole, c) the distance of the charge from the bond, d) the polarity of the reaction medium as quantified by its dielectric constant ε. It is important to note these reflect the impact of a charge on the stability of an isolated species, for assessing the impact of the charge on a reaction barrier or enthalpy one needs such charge effects to change over the course of a reaction so that they do not cancel from the barrier and/or reaction enthalpy.

shown this asymmetry was also a feature in barrier heights of chemical reactions as transition states are generally more polarisable than their reactants or products.[46] These and other studies led to practical take-home messages for designing systems with large pH-switchable effects on bond energies and barrier heights, and these are summarised in Figure 12 for the simple example of a polar R–X bond.

As shown in Figure 12, the nature of the interaction and the alignment of the charge plays a key role in the magnitude of the electrostatic effect. These factors are discussed in more detail in the Companion Tutorial, but as a brief summary, alignment of the charge along the bond axis gives the greatest effect, and orthogonal to it gives the smallest effect. Whether the effect is stabilizing or destabilizing of course depends on the sign of the charge (or equivalently upon which side of the bond the charge is placed). The role of polarizability means that, the more resonance stabilized the species is, and the greater the stabilization. The reverse is true for the charge, however, as delocalisation of the charge weakens the fields experienced by the bond. As a result, within a homologous series, the charge group effects on radical stability were shown to correlate inversely with the spin density on the nominal radical centre (a proxy for how localised the radical was) and correlate positively with the pKa of the acid (a proxy for how unstable the anion is and hence how localised it was likely to be).[45]

While these are defining chemical factors, other aspects are also important. As seen in Figure 12, charge-group effects on stability decay with distance, with simplified relationships predictable by Coulomb's law. For example, a charge dipole interaction decays as $1/r^2$ and a charge quadrupole interaction as $1/r^3$ where r is the distance from the charge to the bond (or more generally the reaction centre). Charge group effects also depend on the polarity of the reaction medium, and this is discussed in more detail below. Importantly, if one is interested in the effect of a charged group on a reaction barrier or enthalpy, then one needs the effect of charge to differ over the course of the reaction so that it does not cancel. For instance, in the case of a bond dissociation energy (BDE), one either needs the charge to stabilize the bond but not the dissociated products, or alternatively stabilize one of the dissociated products but not the bond. The former would lead to an increase in the BDE in the presence of the charge, the latter would lead to a decrease.

4.2 Experimental implementation

The BDE lowering effects described above were discovered computationally but confirmed experimentally via mass spectrometry.[6] In experimentally demonstrating these effects in the gas phase, the thermodynamic cycle in Figure 13 was used. This thermodynamic cycle shows that the effect of forming a negative charge (by deprotonation of HB) on the X–R bond energy of a compound HB…X–R is identical to the difference in HB acidity of HB…X–R and HB…X•. In this way it was possible to measure the effects of negative charges on bond energies without directly measuring the bond dissociation energies of the neutral HB…X–R compounds, which of course are invisible in mass spectrometry. Instead, these BDE differences could be accessed **i**ndirectly by studying relative acidities of HB…X–R and HB…X• using Cook's kinetic method. The mass spectrometry studies confirmed the computational results, with theory replaced by a point charge (i.e. an electric field), thus confirming their electrostatic origin.[6] and experiment in agreement to within an average error of less than 2 kJ mol^{-1}. More importantly they confirmed that remote charged groups, often included as "innocent" charge labels in mass spectrometry, could dramatically influence the results, and hence caution is needed when using them to understand the corresponding neutral systems. The thermodynamic cycle also highlights that electrostatic effects on a reaction energy or barrier from remote charge groups result in equivalent acidity differences between the reactants and transition states and/or products.

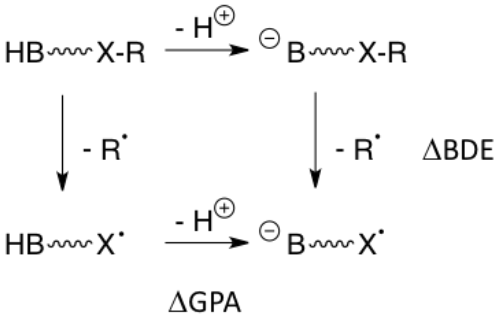

Figure 13. Thermodynamic cycle showing that the change in HB…X–R bond dissociation energy upon deprotonation (ΔBDE) is identical to the difference in acidity of HB of HB…X–R and HB…X• (ΔGPA).

Textbox 2.

According to Coulomb's law, the electrostatic interaction U(r) between charges q_1 and q_2 at distance r is reduced in strength by a dimensionless factor called the *dielectric constant* ε:

$$U(r) = \frac{kq_1q_2}{\varepsilon r}$$

The dielectric constant reflects the polarization of the medium due to induced or permanent dipoles. As a result of their own polarity, molecules of the medium can orient around the charge so as to counteract some of its field lines. As a result, the electrostatic effect of a charged group will be stronger in a solvent of low dielectric constant (such as toluene ε = 2.38 or dichloromethane ε = 8.93) and weak in a solvent of high dielectric constant such as (dimethyl sulfoxide ε = 46.7 or water ε = 80.1).

It should be noted that Coloumb's law is an oversimplification of the problem in a real solvent. This is in part because higher-order terms such as charge-dipole and charge-quadrupole interactions are important, but also because the medium involves real molecules with real geometries and thus factors such as overlap of the solvation shell of individual ions are important, particularly at short range. For a more detailed description of the physics involved see Ref 47.

Whilst the electrostatic effects of charged functional groups are large in the gas phase, these are muted in solution by dielectric screening (see Textbox 2). The extent to which this occurs depends on the polarity of the solvent, with screening being highest in polar solvents such as water and lowest in non-polar solvents such as toluene. Since the solubility of charged groups tends to be highest in polar solvents and lowest in non-polar solvents, experimentally implementing pH-switchable electrostatic catalysis in solution requires a compromise in which some catalysis may be traded to maintain solubility. Nonetheless, significant catalysis in solution is possible, and this was first demonstrated in 2015.[7] In those experiments, carried out in the moderately low polar solvent dichloromethane, the effect of base on the kinetics and thermodynamics of hydrogen atom transfer from the hydroxyl amine of 4-carboxy-TEMPO and a profluorescent nitroxide (PFN) was studied by time-dependent fluorescence spectroscopy (Figure 14). This experiment clearly showed that deprotonation of the carboxylic acid functional group stabilized the 4-carboxy-TEMPO radical and shifted the equilibrium constant of this reaction to the right by a factor of 29 at room temperature, while speeding up the reaction by a factor of 22. Follow-up experiments showed that this electrostatic stabilization of the nitroxide radical meant that in styrene solution in the presence of base, a polystyryl alkoxyamine of 4-carboxy-TEMPO undergoes homolysis and subsequent chain extension at 100°C, while the same compound in the absence of base remains stable under the same conditions (Figure 14).[8] While this pH-switching at 100°C is not especially useful, computational work indicated that further modification of the nitroxide structure could be made so as to allow the same pH-switching of homolysis to occur at room temperature, which would have significant practical applications.[8] At present alkoxyamine homolysis requires much higher temperatures where side reactions occur, lowering the temperature towards room temperature in a controllable manner would potentially reduce these side reactions while also lowering the energy demands of the process.

4.3 Beyond radicals

The initial work on pH-switchable kinetics and thermodynamics focused on radical chemistry, but the concept is equally transferrable to any system where electrostatic effects are important. As proof of concept, a recent computational study explored the effect of charged acid and base groups on the barriers and reaction free energies of Diels-Alder reactions, showing that significant pH switches (up to 60 kJ mol^{-1}) were possible in the gas phase and that a synthetically significant portion remained in solution (ca. 30 kJ mol^{-1} in toluene, ca. 13 kJ mol^{-1} in dichloromethane).[48]

Consistent with earlier theoretical work on the effect of external fields this reaction,[17] aligning the localised electric field perpendicular to the forming and breaking bond and parallel to

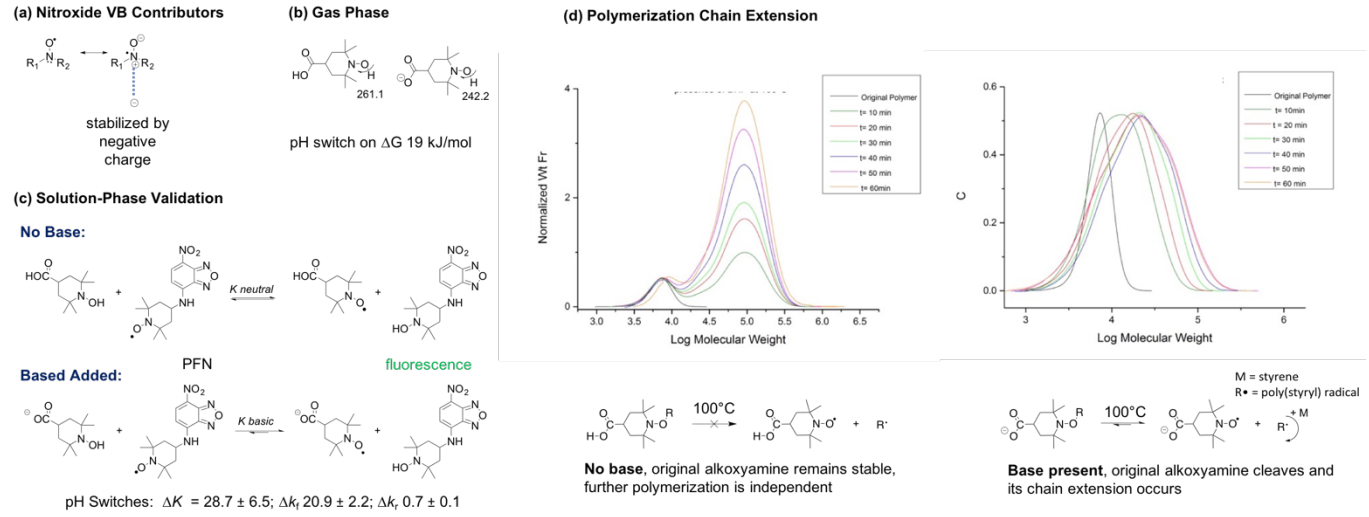

Figure 15. pH-Switchable nitroxide stability. (a) The nitroxide radical is stabilized relative to its parent hydroxylamine and alkoxyamine when a negative charge is aligned along the positive end of the dipole associated with its charge-separated resonance contributors. (b) In the gas phase this leads to a lowering in the bond dissociation Gibbs free energy of 19 kJ mol^{-1} at 298K. (c) In dichloromethane at the same temperature, this results in a shift to the right in the equilibrium constant for the hydrogen atom transfer reaction between hydroxyl amine a profluorescent nitroxide (PFN) of a factor of 28.7, and a corresponding speed up in the forward rate coefficient of 20.9. (d) In practical terms this stabilization means while the polystyryl alkoxyamine of 4-carboxy TEMPO is stable at 100°C, the presence of base allows homolysis to occur so that further polymerization (chain extension) of R-group is possible. This is seen in the polymer molecular weight distributions obtained. In the first case, in the absence of base, the original polymeric akoxyamine (black) remains intact and independent thermal polymerization of styrene occurs; in the second case, identical but with the presence of base, the alkoxymine undergoes homolysis as is evident in the observation that the entire molecular weight distribution grows.

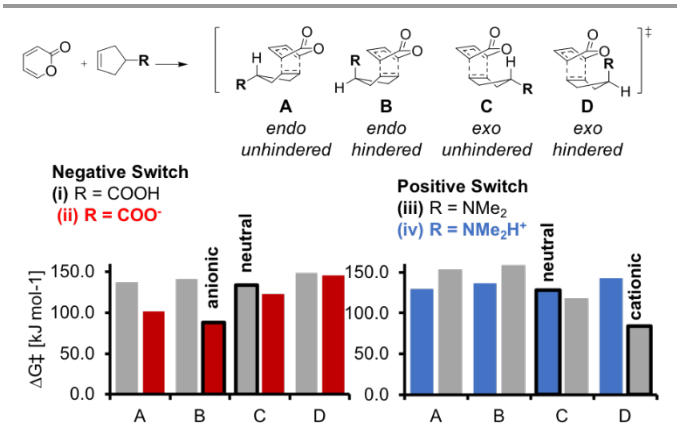

Figure 16. pH-switchable Diels Alder reactions between 2-pyrone and substituted cyclopentadienes, where R represents a pH-switchable functional group. All neutral reactions (grey) favoured the unhindered exo transition state, C. Deprotonation of a carboxylic acid group in basic conditions causes an anionic transition state (red) which favours a hindered endo geometry, B, that is c.a. 45 kJ mol-1 lower in energy than the lowest energy neutral transition state. Protonation of a tertiary amine in acidic conditions causes a cationic transition state (blue) which favours a hindered exo geometry, D, that is again c.a. 45 kJ mol-1 lower in energy than the lowest energy neutral transition state.

the dipole of the diene fragment could switch the regio- and diastereo- selectivity of the major product (Figure 15). Whilst a negative charged group catalysed the endo transition state in the reaction between 2-pyrone and substituted-cycloalkenes, a positively charged group in the same location (effectively switching the direction of the localised electric field), catalysed the exo transition state. Interestingly, the more sterically hindered transition state was preferred for each charged reaction, highlighting that the transition state will align itself to maximise electrostatic stabilisation even at the expense of steric crowding (Figure 15).

4.4 Potential catalyst platforms

To truly harness electrostatic catalysis in bulk solution it is imperative to think beyond placing the charged functional group on the substrate to avoid limiting this chemistry to those systems already carrying the desired acid or base functional group. The next great challenge is to create pH-switchable catalysts, thus moving the charged functional group away from the substrate. This could be envisaged through the inclusion of switchable groups on, for example, organocatalysts. Moreover, tethering such catalysts to polymer supports could potentially assist with the polarity versus solubility trade-off in a manner analogous to enzymes.

One such example of an enzyme-mimicking polymer-based catalyst was recently reported by Connal and co-workers.[49] In this system, an enzyme inspired functional group capable of binding the substrate and catalysing its esterolysis was tethered to a Merrifield resin via “click” chemistry. Hydrophobic chains were also tethered to the same resin and shown to increase the catalytic effect by shielding the active site and decreasing its polarity. While this particular catalyst did not involve specific pH-switching, this type of approach could be adapted for pH-switchable catalysis of other reactions. Other strategies moving forward could include the use of metal-organic frameworks to provide the field and host the reagents in a controlled orientation in that field.

5. Outlook

In summary, while implementation of electrostatic effects in chemistry is not straightforward, we have described three broad experimental platforms in which they have been successfully used. At the single molecule level, OEEFs can be generated within scanning tunnelling microscope (STM) experiments. By attaching reagents to the tip and substrate of the STM, and operating in either blinking or tapping mode, these experiments have the ability to both deliver an OEEF while measuring the effect of its strength and bias on the reaction rate. We have already provided proof of concept experiments for bond forming[9] and bond breaking[11] reactions and based on the extensive theoretical work described in the Companion Tutorial, we expect similar results for many more classes of reaction.

While practical applications of such single molecule experiments are unlikely to expand much beyond high-tech areas such as surface patterning (e.g. Figure 17a), these types of electrical measurements are arguably the gold-standard to guide the trajectory of approaching reactants and to study chemical reactions at the single-molecule level under a precise electric field. One area of intense interest is the biological field and our recent developments in STM technology may make it possible to address the long-standing question: to what extent are electric fields responsible for catalysis in enzymes? As a first step we have developed a method to trap a protein in a tunnelling junction under controlled orientation (Figure 17b).[50] We have used our STM junction approach in the blinking modality together with bioengineering methods that allow the precise localization of chemical groups in the outer protein sphere, so as to specifically connect electrodes and proteins in a STM junction. This approach can be exploited to electrically measure the activity of a redox enzyme, whose catalytic cycle causes changes in the active site’s redox state. Likewise, thanks to the controlled orientation of the trapped protein and its alignment through the tunnelling junction, it is possible to envision that enzymatic activity could be evaluated as a function of an applied OEEF.

Moving beyond the single molecule level, we have also shown that the IFEEs for electrified surfaces can be the effector of chemical change, both in redox and non-redox reactions. This is likely to provide the key platform to take these effects from nano to macro scale. There is already a renaissance in the use of electro-organic chemistry for synthesis,[41] and the recognition that electrostatic catalysis plays a role in chemical changes, that are triggered by electrochemical events, is crucial to understanding and exploiting this growing area. For suitable reactions, the use of electrochemical cells promises a scalable technology that helps to avoid the need for chemicals as catalysts and offers the ability to rapidly switch catalysis on and off. Depending on the system involved, the use of targeted

potentials offers select control over chemical reactions, allowing one to assemble complex molecules in a one pot manner with minimal use of protecting group chemistry.

There is also the obvious possibility of coupling actuation of fluids with chemical reactivity and selectivity (Figure 17c). Transport of reagents in microfluidics relies on electroosmotic flow, which springs from the coupling of electrical double-layer charging and fluid flows in small channels. The reaction environment of microfluidics is intrinsically dominated by surface and electrostatic effects. As such, this could be an ideal platform to demonstrate the immediate implications of electrostatic catalysis in a state-of-the-art chemical processing technology.

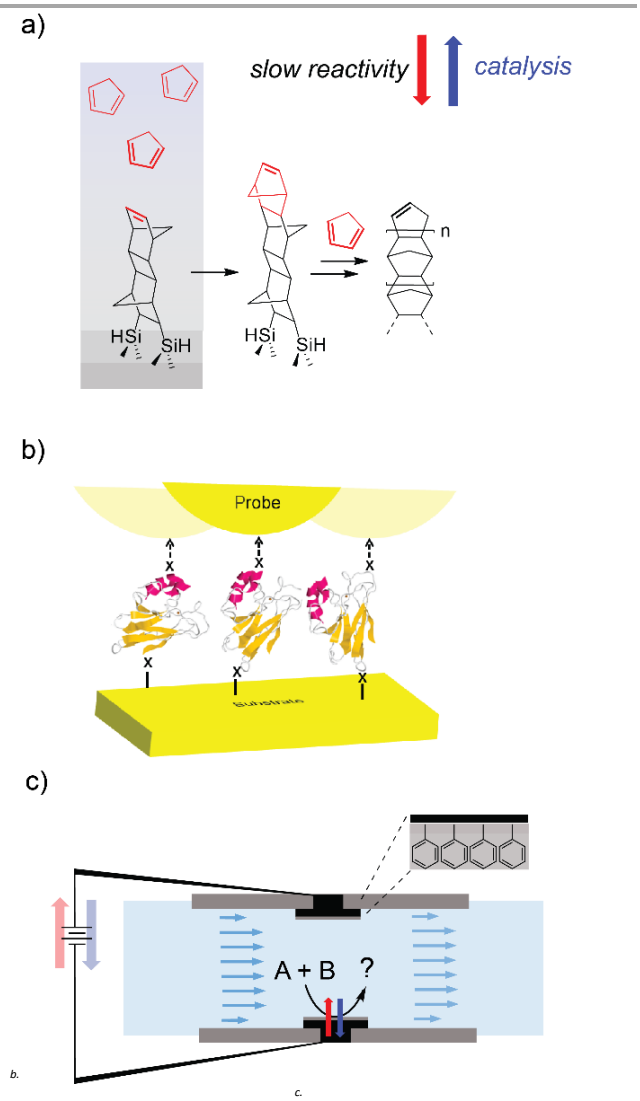

Figure 17. **Outlook**. (a) Using localized high fields on semiconductors[32] may be used to guide the rate of unfavourable surface reactions towards an "electrostatic" lithography where molecules are the ink. (b) Orientation control of a single protein junction through protein bioengineering.[50] This could enable the exploration of field effects on enzymatic reactions and the electrostatic manipulation of catalytic cycles. (c) Turning this knowledge into a device; coupling electroosmotic fluid movements (device actuation) with electrostatic control of chemical reactivity (device efficiency and precision).

Generating static electric fields by friction, known as triboelectricity, offers an exciting prospect for electrostatic catalysis to become a scalable chemical technology. Static charging of insulators has been known since antiquity when it was observed that amber can easily be charged through rubbing and indeed the Greek word for amber is indeed "ielektrónio". Static electricity is on the verge of a renaissance thanks to its scope as a renewable source of energy,[51] and we can envision that Teflon or polyethylene microbeads suspended in a solvent of low dielectric and vigorously "rubbed" in a turbulent fluid or pushed against the walls of the spinning reactor could acquire charges upon contact. Charges would extend inside the hydrocarbon media used to dissolve and suspend reactants and microbeads; it would generate a near-surface field without involving external sources of potential, nor wires or metallic electrodes. This type of contact electrification can be put to use as the effector of electrostatic catalysis and rapidly scaled-up using available fluidic technologies with clear benefits in terms of mass transport of reactant and green credentials.

Finally, turning to the D-LEFs of charged functional groups, there is already proof of concept that, even in solution, these can be used to generate sufficient electric fields to catalyse chemical reactions and manipulate their regio- and stereo-selectivity though simple changes to the pH. While their effects in solution are much smaller than the gas phase, they remain significant under practical solution-phase conditions, and their potential scope is almost infinite.

While the examples provided herein have been selected to reflect systems for which "pure" electrostatic effects are in operation, the importance of electrostatic effects in chemistry is by no-means limited to those situations. Thus, for example, we have shown that coordinated Lewis acids can dramatically catalyse the propagation step of free radical polymerization, and our recognition that electrostatic effects plays a key role in catalysis has allowed us to optimize this system by choosing optimal Lewis acids with higher charges.[52] There is also extensive literature on the role of electrostatics in heterogeneous catalysis.[53] To help exploit the full scope of electrostatic effects, further developments in this space will include the design of catalyst supports, such as polymers and MOFs, the better to allow the catalyst to function in a low polarity environment analogous to Nature.

Conflicts of interest

There are no conflicts to declare

Acknowledgements

M.L.C. gratefully acknowledges the Australian Research Council (ARC) for a Georgina Sweet ARC Laureate Fellowship (FL170100041). S.C. (DE160100732) and N.D. (DE160101101) gratefully acknowledge ARC DECRA Fellowships.

Notes and references

1. E. Gileadi, *Electrode Kinetics for Chemists, Chemical Engineers and Materials Scientists*, Wiley-VCH Verlag GmbH, New York, 1993.
2. S. Shaik, D. Mandal and R. Ramanan, *Nat. Chem.*, 2016, **8**, 1091.
3. A. Warshel, P. K. Sharma, M. Kato, Y. Xiang, H. Liu and M. H. M. Olsson, *Chem. Rev.*, 2006, **106**, 3210.
4. S. D. Fried, S. Bagchi and S. G. Boxer, *Science*, 2014, **346**, 1510.
5. J.-G. Zhou, S. Yang and Z.-Y. Deng, *J. Phys. Chem. B*, 2017, **121**, 11053.
6. G. Gryn'ova, D. L. Marshall, S. J. Blanksby and M. L. Coote, *Nat. Chem.*, 2013, **5**, 474.
7. M. Klinska, L. M. Smith, G. Gryn'ova, M. G. Banwell and M. L. Coote, *Chem. Sci.*, 2015, **6**, 5623.
8. G. Gryn'ova, L. M. Smith and M. L. Coote, *Phys. Chem. Chem. Phys.*, 2017, **19**, 22678.
9. A. C. Aragonès, N. L. Haworth, N. Darwish, S. Ciampi, N. J. Bloomfield, G. G. Wallace, I. Diez-Perez and M. L. Coote, *Nature*, 2016, **531**, 88.
10. G. Reecht, C. Lotze, D. Sysoiev, T. Huhn and K. J. Franke, *J. Phys. Condens. Matter*, 2017, **29**, 294001.
11. L. Zhang, E. Laborda, N. Darwish, B. B. Noble, J. Tyrell, S. Pluczyk, A. P. L. Brun, G. G. Wallace, J. Gonzalez, M. L. Coote and S. Ciampi, *J. Am. Chem. Soc.*, 2018, **140**, 766.
12. Y. B. Vogel, L. Zhang, N. Darwish, V. R. Gonçales, A. Le Brun, J. J. Gooding, A. Molina, G. G. Wallace, M. L. Coote, J. Gonzalez and S. Ciampi, *Nat. Commun.*, 2017, **8**, 2066.
13. C. F. Gorin, E. S. Beh, Q. M. Bui, G. R. Dick and M. W. Kanan, *J. Am. Chem. Soc.*, 2013, DOI: 10.1021/ja404394z.
14. C. F. Gorin, E. S. Beh and M. W. Kanan, *J. Am. Chem. Soc.*, 2012, **134**, 186.
15. B. Borca, T. Michnowicz, R. Pétuya, M. Pristl, V. Schendel, I. Pentegov, U. Kraft, H. Klauk, P. Wahl, R. Gutzler, A. Arnau, U. Schlickum and K. Kern, *ACS Nano*, 2017, **11**, 4703.
16. G. Binnig and H. Rohrer, *Surf. Sci.*, 1983, **126**, 236.
17. R. Meir, H. Chen, W. Lai and S. Shaik, *ChemPhysChem*, 2010, **11**, 301.
18. A. Bellec, M. Cranney, Y. Chalopin, Mayne, G. Comtet and G. Dujardin, *J. Phys. Chem. C*, 2007, **111**, 14818.
19. S.-W. Hla, L. Bartels, G. Meyer and K.-H. Rieder, *Phys. Rev. Lett.*, 2000, **85**, 2777.
20. S. W. Hla, G. Meyer and K. H. Rieder, *ChemPhysChem*, 2001, **2**, 361.
21. D. G. de Oteyza, P. Gorman, Y.-C. Chen, S. Wickenburg, A. Riss, D. J. Mowbray, G. Etkin, Z. Pedramrazi, H.-Z. Tsai, A. Rubio, M. F. Crommie and F. R. Fischer, *Science*, 2013, **340**, 1434.
22. G. P. Salam, M. Persson and R. E. Palmer, *Phys. Rev. B*, 1994, **49**, 10655.
23. Y. Kim, T. Komeda and M. Kawai, *Phys. Rev. Lett.*, 2002, **89**, 126104.
24. S. Pan, Q. Fu, T. Huang, A. Zhao, B. Wang, Y. Luo, J. Yang and J. Hou, *Proc. Natl. Acad. Sci. U.S.A.*, 2009, **106**, 15259.
25. P. Liljeroth, J. Repp and G. Meyer, *Science*, 2007, **317**, 1203.
26. M. Alemani, M. V. Peters, S. Hecht, K.-H. Rieder, F. Moresco and L. Grill, *J. Am. Chem. Soc.*, 2006, **128**, 14446.
27. J. Wirth, N. Hatter, R. Drost, T. R. Umbach, S. Barja, M. Zastrow, K. Rück-Braun, J. I. Pascual, P. Saalfrank and K. J. Franke, *J. Phys. Chem. C*, 2015, **119**, 4874.
28. H. J. Lee and W. Ho, *Science*, 1999, **286**, 1719.
29. J. A. Herron, Y. Morikawa and M. Mavrikakis, *Proc. Natl. Acad. Sci. U.S.A.*, 2016, **113**, E4937.
30. W. Haiss, R. J. Nichols, H. v. Zalinge, S. J. Higgins, D. Bethell and D. J. Schiffrin, *Phys. Chem. Chem. Phys.*, 2004, **6**, 4330.
31. B. Xu and N. J. Tao, *Science*, 2003, **301**, 1221.
32. A. C. Aragonès, N. Darwish, S. Ciampi, F. Sanz, J. J. Gooding and I. Díez-Pérez, *Nat. Commun.* , 2017, **8**, 15056.
33. N. Darwish, A. C. Aragonès, T. Darwish, S. Ciampi and I. Díez-Pérez, *Nano Lett.*, 2014, **14**, 7064.
34. A. C. Aragonès, N. Darwish, W. J. Saletra, L. Pérez-García, F. Sanz, J. Puigmartí-Luis, D. B. Amabilino and I. Díez-Pérez, *Nano Lett.*, 2014, **14**, 4751.
35. A. M. Smith, A. A. Lee and S. Perkin, *J. Phys. Chem. Lett.*, 2016, **7**, 2157.
36. C. C. A. Ng, A. Magenau, S. H. Ngalim, S. Ciampi, M. Chockalingham, J. B. Harper, K. Gaus and J. J. Gooding, *Angew. Chem. Int. Ed.*, 2012, **51**, 7706.
37. P. K. Eggers, N. Darwish, M. N. Paddon-Row and J. J. Gooding, *J. Am. Chem. Soc.*, 2012, **134**, 7539.
38. N. Darwish, P. K. Eggers, S. Ciampi, Y. Tong, S. Ye, M. N. Paddon-Row and J. J. Gooding, *J. Am. Chem. Soc.*, 2012, **134**, 18401.
39. L. Zhang, Y. B. Vogel, B. B. Noble, V. R. Gonçales, N. Darwish, A. L. Brun, J. J. Gooding, G. G. Wallace, M. L. Coote and S. Ciampi, *J. Am. Chem. Soc.*, 2016, **138**, 9611.
40. N. Darwish, M. N. Paddon-Row and J. J. Gooding, *Acc. Chem. Res.*, 2013, **47**, 385.
41. M. Yan, Y. Kawamata and P. S. Baran, *Chem. Rev.*, 2017, **117**, 13230.
42. S. Ciampi, M. James, G. Le Saux, K. Gaus and J. Justin Gooding, *J. Am. Chem. Soc.*, 2012, **134**, 844.
43. W. Lai, H. Chen, K.-B. Cho and S. Shaik, *J. Phys. Chem. Lett.*, 2010, **1**, 2082.
44. A. Salomon, T. Böcking, J. J. Gooding and D. Cahen, *Nano Lett.*, 2006, **6**, 2873.
45. G. Gryn'ova and M. L. Coote, *J. Am. Chem. Soc.*, 2013, **135**, 15392.
46. G. Gryn'ova and M. L. Coote, *Aust. J. Chem.*, 2017, **70**, 367.
47. A. A. Kornyshev, M. A. Vorotyntsev, H. Nielsen and J. Ulstrup, *J. Chem. Soc., Faraday Trans. 2*, 1982, **78**, 217.
48. H. M. Aitken and M. L. Coote, *Phys. Chem. Chem. Phys.*, 2018, DOI: 10.1039/C7CP07562F.
49. M. D. Nothling, A. Ganesan, K. Condic-Jurkic, E. Pressly, A. Davalos, M. R. Gotrik, Z. Xiao, E. Khoshdel, C. J. Hawker, M. L. O'Mara, M. L. Coote and L. A. Connal, *Chem*, **2**, 732.
50. M. P. Ruiz, A. C. Aragonès, N. Camarero, J. G. Vilhena, M. Ortega, L. A. Zotti, R. Pérez, J. C. Cuevas, P. Gorostiza and I. Díez-Pérez, *J. Am. Chem. Soc.*, 2017, **139**, 15337.
51. J. Liu, A. Goswami, K. Jiang, F. Khan, S. Kim, R. McGee, Z. Li, Z. Hu, J. Lee and T. Thundat, *Nat. Nanotech.*, 2018, **13**, 112.
52. J. Y. Jiang, L. M. Smith, J. H. Tyrell and M. L. Coote, *Polym. Chem.*, 2017, **8**, 5948.
53. F. Che, J. T. Gray, S. Ha, N. Kruse, S. L. Scott and J.-S. McEwen, *ACS Catalysis*, 2018, **8**, 5153.

Table of Contents Entry

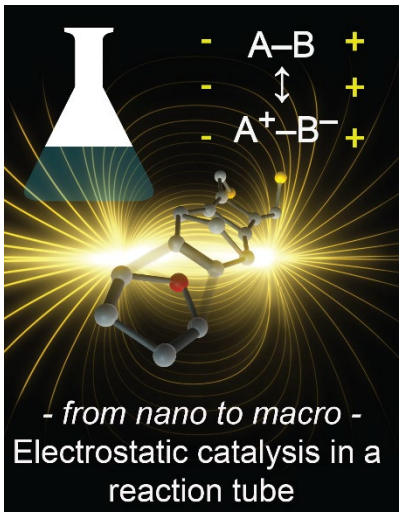

Electrostatic catalysis, once considered theoretical daydreaming, is poised to enter mainstream chemistry, with viable platforms including single molecule experiments, electrified interfaces and pH-switchable charges.